

RESEARCH

Open Access



Self-healing adhesive oxidized guar gum hydrogel loaded with mesenchymal stem cell exosomes for corneal wound healing

Ruoyan Wei^{1,2,4†}, Yunzhe Wang^{1,2†}, Ziqing Feng^{2†}, Rui Liu³, Chang Liu², Xiaojun Hu², Yujia Liu², Bin Kong^{1*}, Xingtao Zhou^{2*} and Meiyang Li^{2*}

Abstract

Hydrogels have shown great potential and value in wound healing. In this study, we construct a mesenchymal stem cell exosomes (MSC-Exos) laden natural biopolymer-based hydrogel with transparent, self-healing, injectable, and tissue adhesive properties to promote corneal regeneration. This hydrogel is synthesized by combining aldehyde-modified oxidized guar gum (OGG) and carboxymethyl chitosan (CMCS) through the dynamic, reversible Schiff base bonds, which endow it with outstanding shear-thinning and self-healing properties, facilitating easy injection through a needle. The physicochemical properties, such as porosity, mechanical strength, and light transmittance, could be precisely tunable by adjusting OGG concentrations. The resultant hydrogel achieves robust tissue adhesion at physiological temperatures due to Schiff base interactions. Besides, the Exos can be uptaken by the corneal epithelial cells and subsequently promote the migration of the cells. We have proven that the MSC-Exos-loaded hydrogel adheres firmly to the defected cornea and significantly improves wound repair by enhancing collagen deposition and reducing inflammation in a rabbit cornea defect model. These results indicated that this multifunctional hydrogel holds immense scientific promise and offers a wide range of clinical applications.

Keywords Hydrogels, Cornea, Tissue adhesive, Mesenchymal stem cell exosomes, Wound healing

[†]Ruoyan Wei, Yunzhe Wang and Ziqing Feng contributed equally to this work.

*Correspondence:

Bin Kong

kongbin13@163.com

Xingtao Zhou

doctzhouxingtao@163.com

Meiyang Li

limeiyang0406073@126.com

¹Department of Biomedical Engineering, School of Medicine, Shenzhen University, Shenzhen 518000, Guangdong, China

²Department of Ophthalmology, Key Lab of Myopia, Eye & ENT Hospital of Fudan University, Ministry of Health, Shanghai 200031, China

³Department of Rheumatology and Immunology, School of Biological Science and Medical Engineering, Nanjing Drum Tower Hospital, Southeast University, Nanjing 210096, China

⁴Zhongshan Hospital Immunotherapy Translational Research Center, Shanghai Medical College, Shanghai 200031, China

Introduction

Corneal injury, one of the most common types of ocular damage, can result in severe complications such as corneal perforation, scarring, and ultimately significant vision impairment in the absence of prompt and effective treatment [1–3]. Traditional management of severe corneal defects relies on corneal transplantation [4]; however, this approach faces challenges, like donor shortages, risks of graft rejection, and potential dehiscence [5, 6]. Ideal corneal substitutes must exhibit transparency, appropriate mechanical strength, strong tissue adhesion, and the ability to promote both epithelial and stromal regeneration. Hydrogels have emerged as promising alternatives for corneal repair due to their unique properties, including high moisture content, tunable



porosity, and the ability to mimic the extracellular matrix microenvironment [3, 7, 8]. Hydrogels are primarily fabricated from either natural biopolymers (e.g., gelatin, hyaluronic acid, and chitosan), or synthetic polymers (e.g., cyanoacrylate, polyethylene glycol, and polyvinyl alcohol) [9–11]. While these hydrogels functionalized with bioactive components (e.g., growth factors and proteins) show therapeutic potential in wound healing [12, 13], they often fail to meet all essential requirements for corneal repair. Natural biomaterials may lack sufficient tissue adhesion whereas synthetic materials may exhibit poor biocompatibility. To address these limitations, this study seeks to answer a critical question: How can a multifunctional hydrogel be engineered to fulfill all necessary properties for corneal healing and enhance in-situ wound repair? We hypothesized that a synergistic combination of dynamic covalent chemistry and bioactive exosome delivery could create an optimal microenvironment for corneal regeneration, addressing both the mechanical and biological challenges of current approaches.

Based on the requirements for an ideal corneal substitute, we designed a multifunctional hydrogel by linking natural biopolymers through Schiff base reactions, with exosomes incorporated to enhance therapeutic efficacy, as illustrated in Fig. 1. While carboxymethyl chitosan (CMCS) has been widely applied in hydrogel preparation [14, 15], its combination with oxidized guar gum (OGG) remains scarcely investigated. This study leverages the synergistic effect between CMCS and OGG to endow hydrogels with unique self-healing properties and enhanced mechanical strength, thereby broadening the biomedical applications of CMCS-based hydrogels. Although CMCS-based hydrogels have been utilized in wound healing, this research pioneers their design as a specialized carrier for non-invasive corneal repair. The hydrogel's self-healing and adhesive properties enable it to conform precisely to the corneal surface, forming a stable protective layer that mitigates external irritation and friction-induced damage, offering a novel solution for minimally invasive corneal trauma treatment. Mesenchymal stem cell-derived exosomes (MSC-Exos) exhibit anti-inflammatory and pro-healing properties [16, 17], yet their delivery efficiency is constrained by traditional sustained-release carriers. The CMCS-based hydrogel developed in this study, through Schiff base reaction-induced dynamic networks, enables the controlled exosome release, providing a new delivery platform for extracellular vesicles in clinical applications.

In this study, we fabricated composite MSC-Exos-incorporated hydrogels, exhibiting transparent, self-healing, injectable, and tissue adhesive properties, aimed at facilitating corneal regeneration. The hydrogels formed via reversible Schiff base interactions between aldehyde groups on the aldehyde-modified OGG chain and amino

groups on the CMCS chain. By adjusting OGG concentrations, the porosity, mechanical properties, and light transmittance of the hydrogel were controllable. The hydrogels demonstrated robust self-healing and shear-thinning characteristics, enabling easy injection via a needle, and achieved strong tissue adhesion at physiological temperatures through Schiff base interactions between aldehyde groups in the hydrogel and amino groups in the cornea. The hydrogel also exhibited excellent biocompatibility and could promote the proliferation of corneal cells. The loaded MSC-Exos could be taken up by the corneal epithelial cells and subsequently promote their migration. In a rabbit corneal defect model, the MSC-Exos encapsulated hydrogel was demonstrated to tightly adhere to the corneal defect area and facilitate corneal wound healing by promoting epithelium and stroma regeneration, inhibiting scarring, and mitigating inflammation. Therefore, we believe that our multifunctional hydrogel holds significant scientific importance and promising clinical applications.

Results

OGG synthesis was achieved through GG oxidation using sodium periodate (NaIO_4). Structural confirmation was obtained through ^1H nuclear magnetic resonance (^1H NMR) and Fourier transform infrared spectroscopy (FTIR) analyses. The ^1H NMR spectrum revealed a characteristic aldehydic proton peak at 9.3 ppm (Figure S1(a)). The FTIR spectrum of pure GG (Figure S1(b)) revealed typical peaks at 3400 (O–H), 2910 (C–H), 1152 (C–O), and 1002 cm^{-1} (glycosidic linkage of the GG pyranose ring). After the reaction of GG with NaIO_4 , a new peak was observed at 1727 cm^{-1} , corresponding to the aldehyde symmetrical vibration. The aldehyde groups of the monomeric sugar units and the OH groups of the unoxidized ring residue can form a hemiacetal bond via the chemical reaction, which likely accounts for the relatively weak intensity of aldehyde group signals. Similarly, CMCS synthesis was verified through comparative ^1H NMR and FTIR analyses of CS and CMCS. The ^1H NMR spectrum showed characteristic peaks at 3.2–3.5 ppm for H-2 protons of carboxymethyl groups (Figure S1(c)). FTIR analysis revealed significant modifications in the chemical structure, where the characteristic amino group bending vibration at 1550 cm^{-1} and C–O–C asymmetric stretching at 1242 cm^{-1} in pristine CS were accompanied by a new absorption band at 1422 cm^{-1} in CMCS, corresponding to the asymmetric stretching vibration of carboxylate groups (Figure S1(d)). These spectral features collectively demonstrate the successful introduction of carboxymethyl groups onto the chitosan backbone, confirming the synthesis of CMCS.

The fabrication of OGG/CMCS hydrogel involved simple mixing of OGG and CMCS solutions as the aldehyde

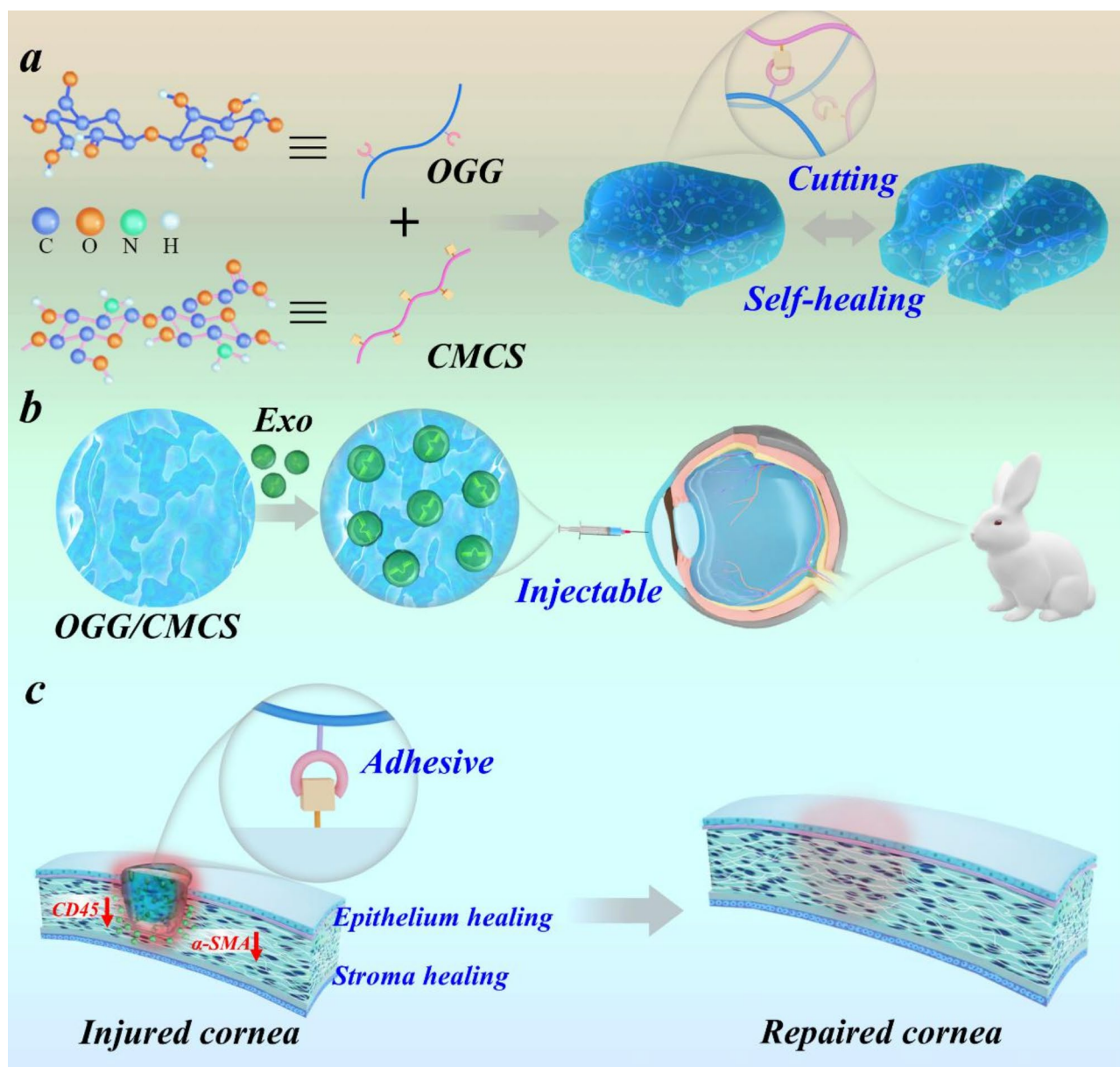


Fig. 1 Schematic illustration of the synthesis and characteristics of MSC-Exos-loaded OGG/CMCS hydrogels. **(a)** Synthesis of OGG/CMCS hydrogels and their self-healing properties. **(b)** Application of MSC-Exos-loaded OGG/CMCS hydrogels in corneal wound healing. **(c)** The hydrogel exhibits robust tissue adhesion during corneal regeneration, effectively mitigating inflammation and suppressing fibrosis

group of OGG can form reversible Schiff base bonds with the amino group of CMCS. Hydrogels prepared by 1.5 wt% CMSC and varying concentrations of OGG (2.0 wt%, 1.5 wt%, and 1.0 wt%) were used to perform the in vitro physiochemical properties characterization. The microstructure of the hydrogels was characterized by observing freeze-dried samples using scanning electron microscopy (Figs. 2(a)–2(c)). Variations in the formulation of the hydrogel were found to impact its porosity. Specifically, the OGG/CMCS-2.0% hydrogel demonstrated smaller pore sizes and a denser network structure in comparison

to the OGG/CMCS-1.5% and OGG/CMCS-1.0% (Figure S2).

Additionally, good homogeneity of the hydrogel plays a crucial role in enhancing its mechanical strength, while also providing a more suitable environment for cell adhesion and proliferation [18]. Consequently, dynamic rheology analysis was conducted on OGG/CMCS hydrogels with different formulations to further investigate these properties. For each hydrogel, its storage modulus (G') exceeded the loss modulus (G'') consistently, signifying that the hydrogel was free-standing (Fig. 2(d)). The modulus–strain curves demonstrated that under strains

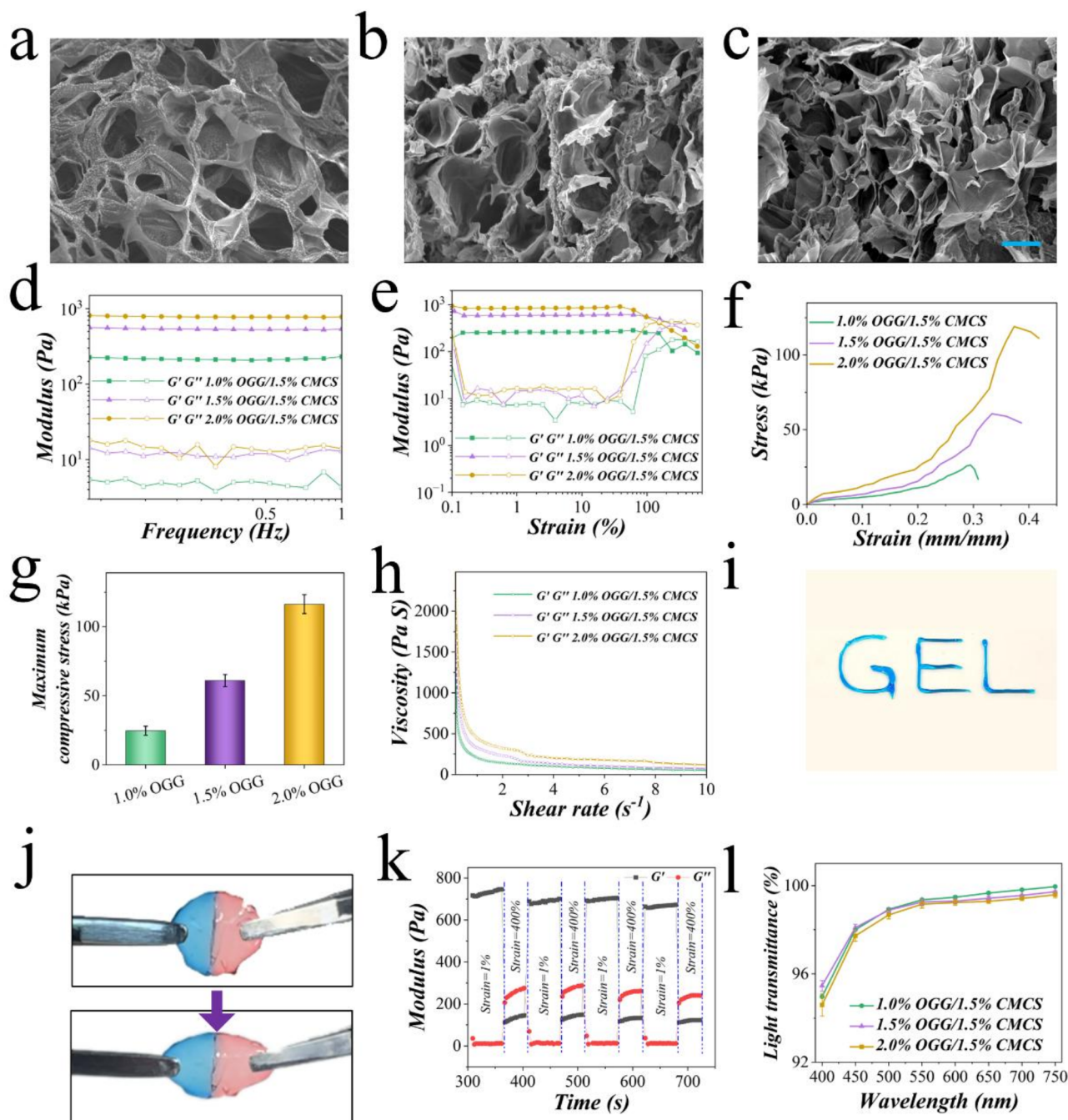


Fig. 2 Fabrication and characterization of the OGG/CMCS hydrogels. (a)–(c) Scanning electron microscopy images depicting OGG/CMCS hydrogels with OGG concentrations of 1.0% (a), 1.5% (b), and 2.0% (c), respectively. Scale bar: 20 μm . (d)–(e) Frequency-dependent (d) and strain-dependent (e) rheology analysis of the hydrogels. (f) Compressive stress-strain profiles of the hydrogels. (g) Histogram of the maximum compressive stress of hydrogels. (h) Viscosity changes in hydrogels with increasing shear rates. (i) Injectability and extrudability of the hydrogel through a syringe. (j) Stretchability assessment of the hydrogel. (k) Variation of G' and G'' with time during continuous step strain measurement in 1% and 400% strain cycles. (l) Light transmittance of the hydrogels across wavelengths from 400 to 750 nm.

less than 100%, the modulus of all hydrogels remained steady, with G' surpassing G'' , suggesting the network structure was stable within the range (Fig. 2(e)). As strain increased, the G' declined, ultimately falling below G'' , indicating the breakdown of the network structure.

Besides, the OGG/CMCS-2.0% demonstrated the highest yielding modulus, whereas OGG/CMCS-1.0% exhibited the lowest yielding modulus, indicating a correlation between the mechanical properties and microscopic structures of the hydrogel. The compressive mechanical

properties of the hydrogels were quantitatively evaluated, as illustrated in Figs. 2(f) and 2(g). A concentration-dependent enhancement in compressive strength was observed, with OGG/CMCS-2.0% exhibiting the highest maximum compressive strength, followed by OGG/CMCS-1.5%, while OGG/CMCS-1.0% demonstrated the lowest mechanical strength. This trend aligns with the rheological measurements.

Self-healing injectable hydrogels have extensive applications, including drug delivery and tissue regeneration [19], and offer a solution for the repair of an irregular-shaped corneal wound. Consequently, we assessed the rheological characterization of the OGG/CMCS hydrogels. All formulations exhibited pronounced shear-thinning behavior, with viscosity decreasing as shear rates increased under a constant 1% strain (Fig. 2(h)), indicating excellent injectability. This rheological property enables smooth extrusion through 25-gauge needles while maintaining structural integrity, as demonstrated in Fig. 2(i), without clogging. To confirm the self-healing capability of OGG/CMCS hydrogels, we fabricated two shell-shaped hydrogels containing pink and blue dyes (Figure S3). The hydrogels were cut with a blade into two half pieces, and one half containing pink dye was closely brought into contact with the one containing blue dye. After 2 hours, the two halves seamlessly healed into a unified structure, capable of supporting its weight under gravity (Figure S3). The healed unit also demonstrated the ability to withstand stretching up to almost twice its original length without rupturing (Fig. 2(j)). Moreover, continuous oscillatory step-strain measurements were conducted to test the rheological self-healing properties. During the test, the oscillatory strain transitioned from 1% over an 80-second interval to 400% over a 60-second interval, with a total of four cycles. When the strain reached 400%, G' became less than G'' , indicating hydrogel breakage. Yet, G' promptly returned to the initial value as the strain reverted to 1%, surpassing G'' (Fig. 2(k)). The observed self-healing capability facilitates both smooth injection through narrow-gauge needles and effective integration with corneal defects, enabling minimally invasive repair.

Notably, achieving high transparency in visible light is crucial for a corneal patch to avoid hindering vision during corneal repair. Thus, the light transmittance of OGG/CMCS hydrogels was evaluated on different wavelengths (Fig. 2(l)). All hydrogel samples with different formulations exhibited remarkable transparency, although the transmittance experienced a slight decrease with the increase in OGG concentration. The swelling and degradation characteristics of OGG/CMCS hydrogels were also evaluated. The OGG/CMCS-2% formulation demonstrated lower swelling capacity (Figure S4(a)) and slower degradation (Figure S4(b)) during incubation in

PBS compared to both OGG/CMCS-1.5% and OGG/CMCS-1% hydrogels, suggesting a concentration-dependent behavior.

Furthermore, the OGG/CMCS hydrogels demonstrated effective tissue adhesive properties. The green-dye-containing hydrogels were in situ formed on porcine skin, displaying robust adherence under stretch, distortion, and bending (Fig. 3(a)). After immersing in water, the hydrogels could still adhere to porcine skin, even under distortion (Figure S5). This suggests a robust tissue-binding capacity of the hydrogel. Further comparisons of adhesiveness among different formulations were conducted through wound closure and lap shear tests. The OGG/CMCS-2% hydrogel demonstrated significantly higher adhesion strength (33.5 ± 2.78 kPa) than both OGG/CMCS-1.5% (26.7 ± 2.25 kPa, $p < 0.05$) and OGG/CMCS-1% hydrogels (20.7 ± 1.76 kPa, $p < 0.01$) (Fig. 3(b)). Similarly, OGG/CMCS-2% hydrogel demonstrated significantly higher shear strength (7.1 ± 0.4 kPa, $p < 0.01$) and OGG/CMCS-1% hydrogel (4.2 ± 0.3 kPa, $p < 0.001$) (Fig. 3(c)), suggesting the adhesive properties exhibited a concentration-dependent behavior.

To assess biocompatibility, the liquid extracted from the OGG/CMCS hydrogel was utilized for culturing human corneal epithelial cells (HCECs) and keratocytes (HKs). Cells were cultured with hydrogel extracts (0, 5, 10, and 20 mg/mL) separately and cell viability was evaluated on days 1, 2, and 3 using the CCK-8 assay. On day 2, the viability of HCECs in extract liquid at all three concentrations was significantly higher than the control (normal medium), and the viability of HKs in extract liquid at 20 mg/mL was significantly higher than the control (Figs. 4(a) and 4(b), all $p < 0.05$). The viability remained high for 3 days, indicating the hydrogel's robust biocompatibility. Compared to other self-healing hydrogels and related hydrogel systems for corneal regeneration, our work exhibits relatively strong mechanical strength, robust adhesion, and excellent cytocompatibility [20–24] (Figure S6).

To evaluate the quality of MSC-Exos, their concentration was quantified using nanoparticle tracking analysis (NTA), revealing an original concentration of 7.3×10^{10} particles/mL (Fig. 4(c)). Furthermore, the morphology of MSC-Exos was observed via transmission electron microscopy (TEM). The acquired Exos exhibited a characteristic saucer shape, featuring small vesicles with a central depression, in line with prior observations (Fig. 4(d)). Furthermore, the MSC-Exos expressed CD9 and CD63 exosomal markers (Fig. 4(e)). Following a 12-hour co-culture of MSC-Exos with HCECs, Exos effectively entered HCECs, indicating their easy endocytosis or internalization by HCECs (Fig. 4(f)). Additionally, the biological impact of MSC-Exos incorporated

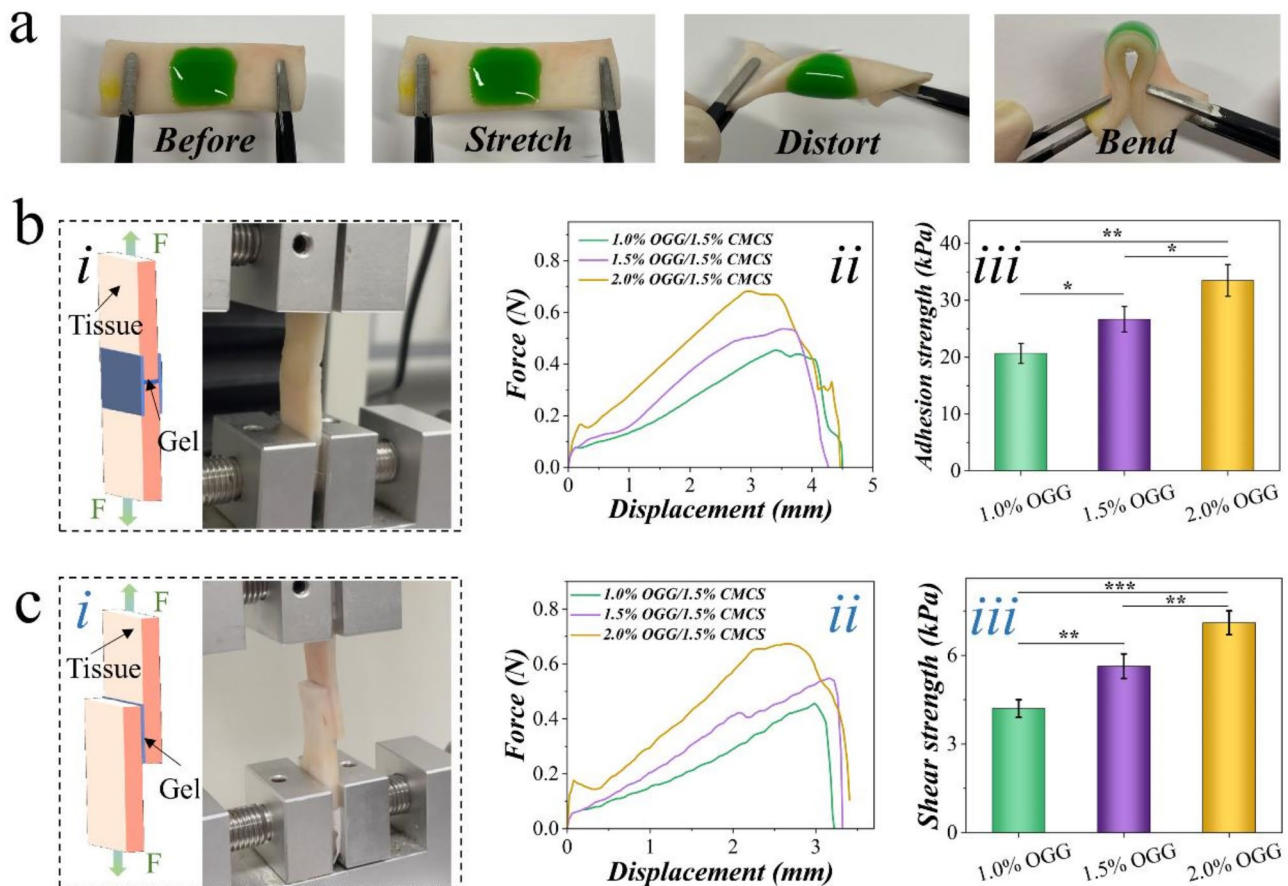


Fig. 3 Adhesion properties. (a) Photographs of OGG/CMCS hydrogels adhered to porcine skin tissue. The hydrogel remains intact without detachment or cracking with the tissue, even during stretching, distorting, or bending. (b)–(c) Tissue adhesive properties of the hydrogels: (i) schematic representation and photography of the test; (ii) force-displacement curves; (iii) histogram of the adhesion (b) and shear strength (c) ($p < 0.05$, $**p < 0.01$, $***p < 0.001$)

OGG/CMCS hydrogel on HCECs was investigated using a wound healing assay (Fig. 4(g)–4(h)). We detected a significant enhancement in scratch closure at 12 and 24 h with the application of MSC-Exos-loaded hydrogel compared to the control ($p < 0.001$). These results suggest that MSC-Exos maintains long-term activity for the promotion of corneal epithelium migration in our hydrogel.

The release profile of exosomes from the OGG/CMCS hydrogel was shown in Fig. 4(i), indicating a sustained and slower release of OGG/CMCS-2% hydrogel than OGG/CMCS-1.5% and OGG/CMCS-1% for 72 h after encapsulation of exosomes.

After in vitro characterization and assessment of the OGG/CMCS hydrogels, we selected the hydrogel formulation with 2.0% OGG and 1.5% CMCS to assess its performance in vivo due to its superior mechanical strength, tissue adhesive properties, slower swelling rate, and controlled release of exosomes. We implanted the OGG/CMCS hydrogel subcutaneously in mice for 4 weeks to evaluate its in vivo biocompatibility. Histological examination showed that OGG/CMCS hydrogel implantation caused no lesions in the heart, liver, spleen, lung, or

kidney in comparison to mice in the control group (Figure S7).

A rabbit corneal defect model was then used to evaluate the treatment effects. The amount of exosome encapsulation in the hydrogel is 8.75×10^9 particles/mL. The corneal defect was treated with the MSC-Exos-loaded OGG/CMCS hydrogel, pure hydrogel, and MSC-Exos respectively, while an untreated group was used as the control (Fig. 5(a)). After gelation, both hydrogels with and without MSC-Exos adhered effectively to the defected area, exhibiting smooth surfaces (Fig. 5(b)). The defected area was monitored in four groups at 1, 2, 4, and 8 weeks (Figs. 5(c)–5(e), Figure S8). Corneal transparency and the integrity of the corneal surface were assessed using diffuse illumination and a narrow slit beam. The corneal defect area remained smooth and transparent in eyes treated with MSC-Exos-loaded OGG/CMCS hydrogel during the 8 weeks post-surgery, while it exhibited mild opacity in the control and pure hydrogel groups at the 8th week (Figs. 5(c)–5(e)). Further, fluorescein staining was utilized to observe the corneal re-epithelialization. On the 7th day after surgery, eyes treated with

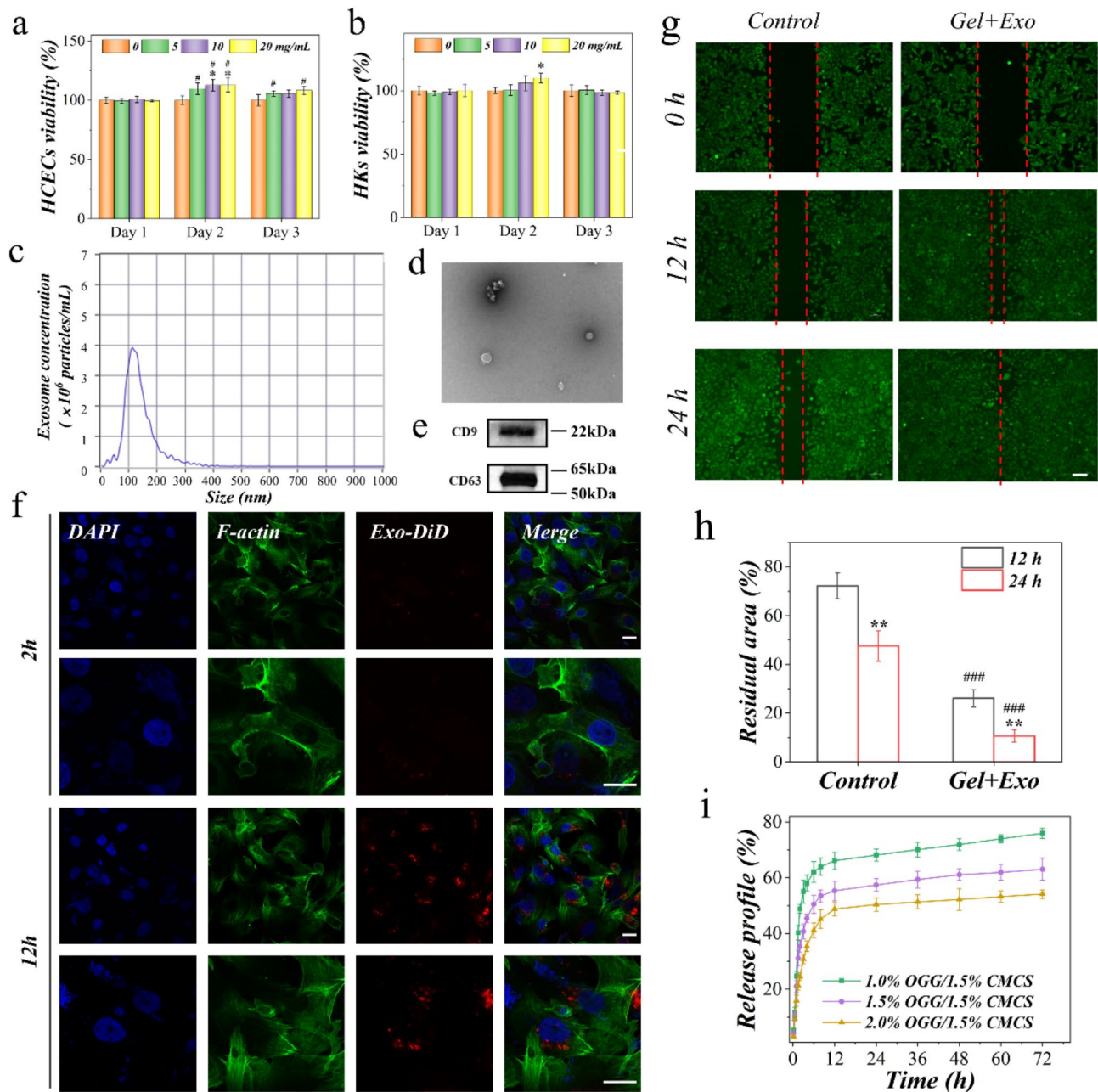


Fig. 4 Biocompatibility of OGG/CMCS hydrogels and biological activity of mesenchymal stem cell exosomes (MSC-Exos) in the hydrogels. **(a–b)** Cell viability of human corneal epithelial cells (HCECs, **a**) and keratocytes (HKs, **b**) cultured with different concentrations of hydrogel patch extract following 1, 2, and 3 days ($*p < 0.05$ vs. control group; $\#p < 0.05$ vs. Day 1 within the same treatment group). **(c)** Size distribution profile of exosomes (following 1000-fold dilution). **(d)** Transmission electron microscopy of MSC-Exos. Scale bar: 200 nm. **(e)** Western blot analysis of the exosome surface markers. **(f)** Confocal microscopy of cellular uptake of DiD-labeled MSC-Exos by HCECs after culturing for 2 h and 12 h. Scale bar: 20 μ m. **(g)** Scratch wound assay. Representative micrographs of HCECs treated with MSC-Exos-loaded OGG/CMCS hydrogel for 0, 12 h, and 24 h. Scale bar: 100 μ m. **(h)** Quantitative evaluation of the scratch wound using ImageJ ($**p < 0.01$ vs. 12 h within the same treatment group; $###p < 0.001$ vs. control group). **(i)** Release profile of exosomes from the OGG/CMCS hydrogel

MSC-Exos-loaded OGG/CMCS hydrogel exhibited minimal detection of green fluorescent staining in the epithelial defect area, contrasting with the relatively larger staining observed in the other groups (Fig. 5(c)), suggesting the novel hydrogel's potential to enhance corneal epithelium healing. Anterior segment OCT was used to

evaluate the process of hydrogel degradation and wound healing. The hydrogel displayed varying light reflectivity compared to the corneal stroma in OCT. The healing process occurred as the hydrogel gradually degraded and the healing was notably accelerated in the eyes treated with the MSC-Exos-loaded OGG/CMCS hydrogel

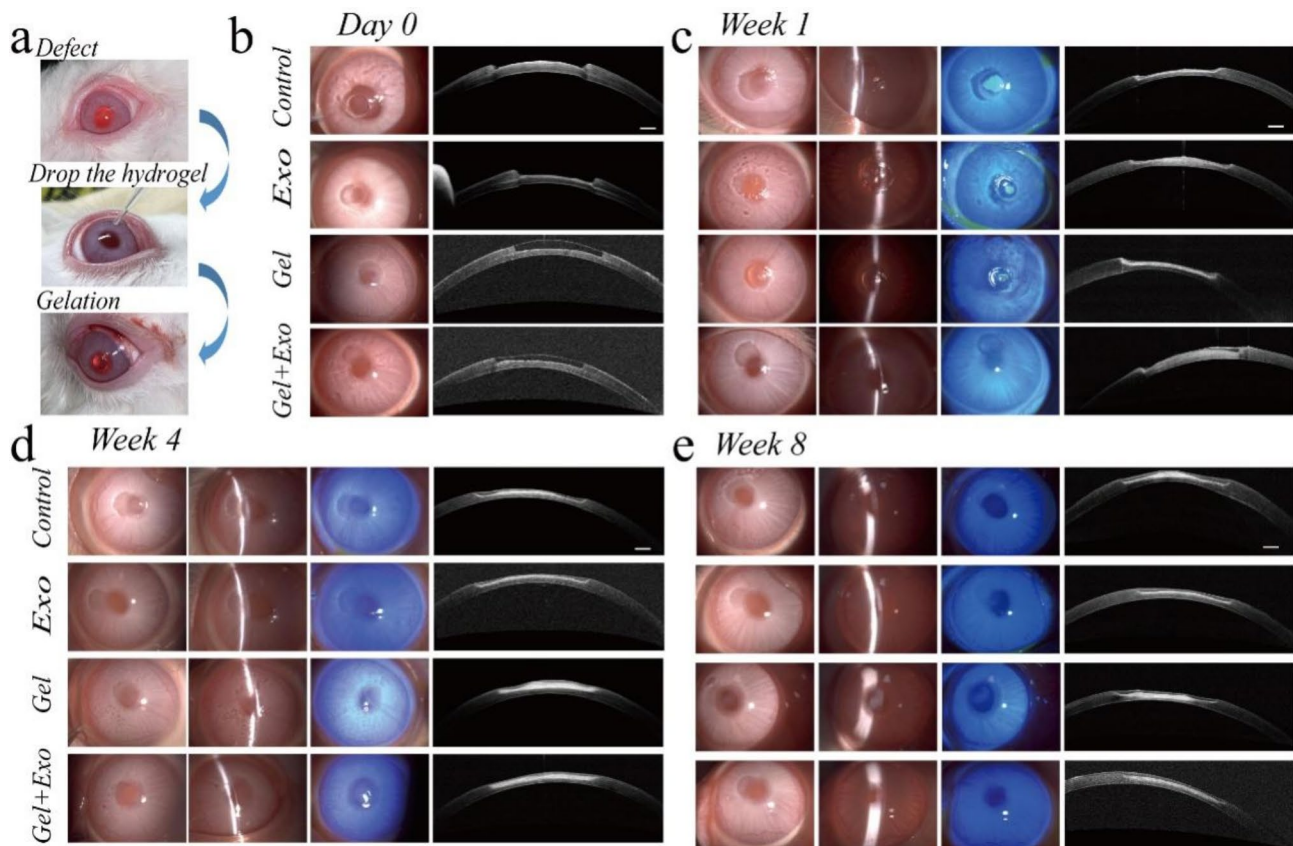


Fig. 5 In vivo assessment of the MSC-Exos-loaded OGG/CMCS hydrogels in a rabbit corneal defect model. **(a)** Operation steps. **(b)–(e)** Representative slit lamp photos (diffuse illumination, narrow slit beam, and sodium fluorescein staining) and optical coherence tomography (OCT) images immediately **(b)**, 1 **(c)**, 4 **(d)**, and 8 **(e)** weeks after surgery. Scale bar: 500 μm

compared to the other groups (Figs. 5(c)–5(e) and Figure S8). The hydrogel eventually degraded completely, leaving no permanent material in the cornea.

Besides, histological examinations at 4 and 8 weeks revealed corneal repair in the defect area (Fig. 6(a)). In eyes treated with the MSC-Exos-loaded OGG/CMCS hydrogel, the thickness of epithelium and stroma in the defect area closely resembled that of the surrounding cornea, and the ratio of corneal stroma thickness to epithelial thickness was significantly greater than that in eyes without treatment and eyes treated with pure OGG/CMCS hydrogel on week 8 (Fig. 6(b)). Meanwhile, the recovery rate of overall corneal thickness on week 8 was highest in eyes treated with Exos-loaded hydrogel (Fig. 6(c)). In contrast, the control and pure hydrogel groups exhibited epithelial overgrowth, yet the stromal layer and the overall corneal thickness were significantly smaller compared to normal conditions. The precise arrangement of collagen fibrils in stroma is crucial for maintaining corneal clarity and optimal stromal hydration [1]. Masson trichrome staining illustrated that in the eyes treated with MSC-Exos-loaded OGG/CMCS hydrogel, the stroma maintained a well-arranged lamellar structure in contrast

to the eyes treated with pure hydrogel (Fig. 6(a)). The cornea treated with Exos-loaded OGG/CMCS hydrogel exhibited higher coverage of collagen fiber (blue) in the corneal stroma compared to the Exos and pure hydrogel groups (Fig. 6(d)), indicating its potential to promote collagen fiber regeneration, while significant fibrosis (red) was observed in the repaired corneal stroma of Exos and pure hydrogel groups. It may contribute to better corneal transparency following healing with the assistance of the exosomes-loaded hydrogel.

Additionally, immunofluorescence staining for alpha-smooth muscle actin (α -SMA) and CD45 was utilized to evaluate the local fibrosis and inflammatory response in week 4. (Figs. 6(e) and 6(f)). The untreated wounded cornea exhibited higher expression of α -SMA at the wound edge compared to the cornea treated with MSC-Exos-loaded OGG/CMCS hydrogels (Fig. 6(e)). Activated keratocytes near the wound surface likely underwent differentiation into α -SMA-positive myofibroblasts in the injured cornea [25]. Exosome-loaded hydrogels significantly reduced α -SMA expression, demonstrating their potential to prevent myofibroblast formation and corneal scarring. Leukocyte infiltration, as indicated by

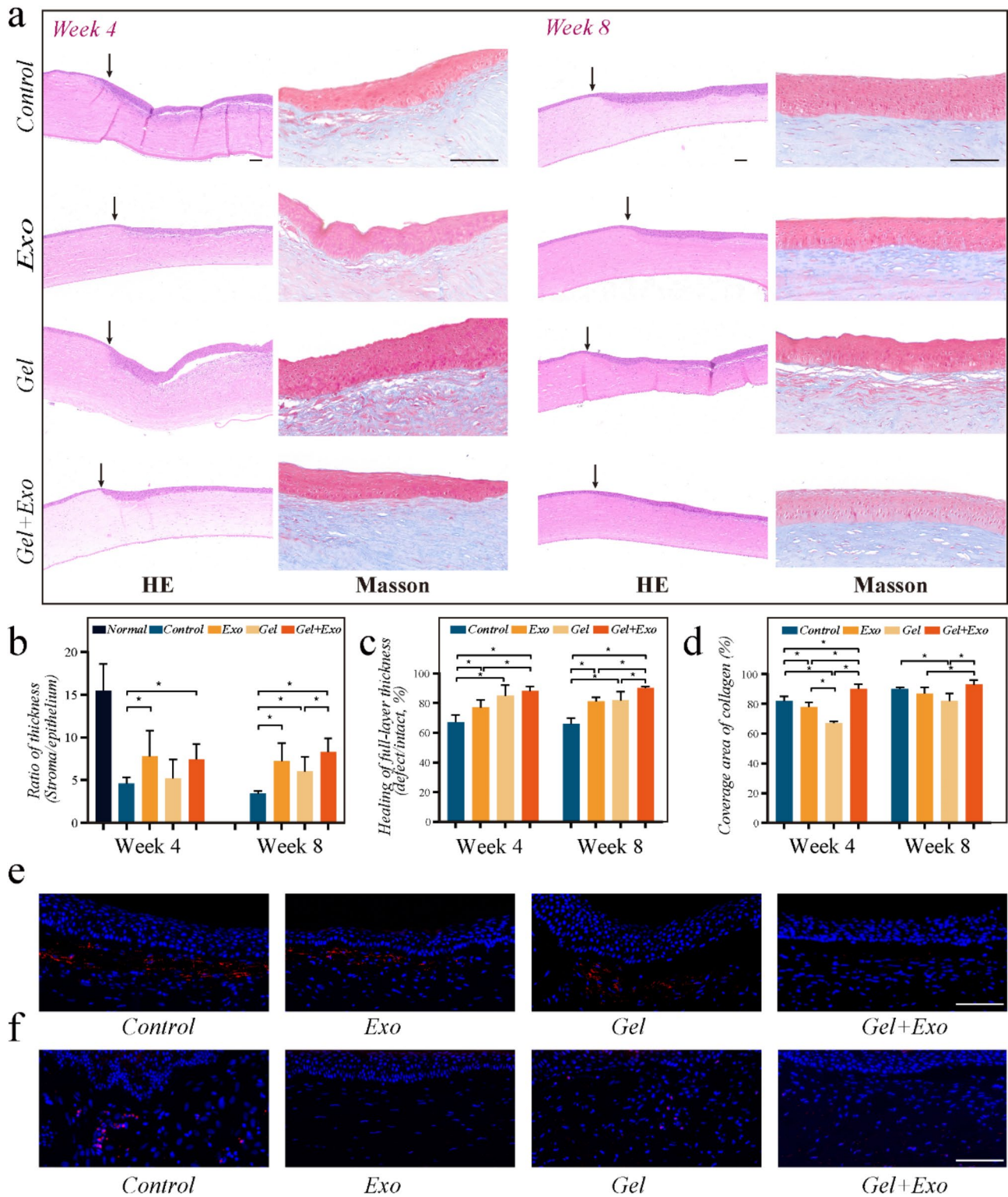


Fig. 6 Histological evaluation of operated corneas. **(a)** HE and Masson staining on week 4 and 8 (arrows indicate the boundary of the corneal defect). Scale bar: 100 μ m. **(b)** Ratio of corneal stroma thickness to epithelial thickness. **(c)** Recovery of corneal thickness. **(d)** Coverage area of collagen in corneal stroma. **(e-f)** Immunofluorescent staining of α -SMA **(e)** and CD45 **(f)** on week 4. Scale bar: 100 μ m. (* $p < 0.05$)

CD45 expression, was lower in the cornea defects treated with exosome-loaded OGG/CMCS hydrogels in contrast to the control and pure hydrogel groups, suggesting the ability of exosome-loaded hydrogels to mitigate inflammation during corneal regeneration (Fig. 6(f)). The findings indicated that the MSC-Exos-loaded OGG/CMCS hydrogel can provide an ideal environment to enhance corneal wound healing in vivo.

Discussion

The cornea is susceptible to damage from both external and internal factors, potentially resulting in vision loss. An ideal approach to corneal regeneration should address both structural and functional restoration [26]. Hydrogels are known for their good biocompatibility and ability to support tissue regeneration, but pure hydrogels often show insufficient repair efficiency and fail to achieve adequate transparency in the regenerated cornea. Exosome therapy can reduce inflammation, remodel scar tissue, and enhance healing, but its application is constrained by the requirement for frequent administration. In this study, we combined OGG/CMCS hydrogels with MSC-Exos, successfully achieving corneal regeneration both structurally and functionally.

The selection of OGG/CMCS hybrid hydrogel was based on its unique optical, mechanical, and biological properties, making it well-suited for corneal wound healing. Since corneal transparency is essential for vision, it is crucial to prioritize light transmittance when developing corneal substitutes [27]. Many hydrogel-based materials, while effective for structural regeneration, often compromise on transparency, which would limit their use in corneal therapy. Our result showed that OGG/CMCS exhibited excellent transparency, addressing this concern. Tissue adhesion is crucial to prevent detachment of the substitutes from the cornea and our results suggested robust adherence of OGG/CMCS hydrogels to both porcine skin and cornea. This strong adhesion is attributed to the reversible Schiff base bonds between the aldehyde group of hydrogel and the amino group of tissue [28]. Additionally, the OGG/CMCS hydrogel's structure, formed through reversible Schiff base bonds between the aldehyde group of OGG and the amino group of CMCS [29, 30], confers self-healing and injectable properties, as demonstrated in our study. The in vivo results indicate the hydrogel's ability to conform to deep corneal defects thoroughly, and it holds promise for future use in treating corneal defects that may differ in size and shape.

The structure restoration of corneal defects involves the regeneration of corneal epithelium and stroma. Corneal epithelial healing is a complex and coordinated physiological process involving cell migration, proliferation, adhesion, and differentiation [13]. In this study, the OGG/CMCS hydrogels demonstrated good

biocompatibility both in vitro and in vivo. At certain concentrations, the OGG/CMCS hydrogel was shown to enhance corneal epithelium proliferation, as evidenced by CCK8 assay results. This effect may be partly attributed to the hydrogel components, as both GG and chitosan are naturally derived biopolymers that support cellular proliferation [31, 32], although the effect was gradually depleted over time. The scratch wound assay further demonstrated that the combination of OGG/CMCS and MSC-Exos effectively accelerates epithelial migration. Additionally, corneal sodium fluorescein staining in the rabbit model showed that this combination could assist in corneal epithelial regeneration without the need for frequent eye medication.

For the regeneration of the corneal stroma, it is crucial to restore both corneal thickness and transparency. The precise arrangement of collagen fibrils in stroma is vital for maintaining corneal clarity and optimal stromal hydration [1]. During corneal wounds, quiescent keratocytes become mitotic and differentiate into fibroblasts and myofibroblasts, depositing proteins to repair the ECM; however, corneal opacity may occur [33]. Consequently, a key objective in therapy development is to prevent corneal scarring and fibrosis. MSC-Exos have demonstrated their ability to modulate inflammation, promote tissue regeneration, and remodel scar tissue [34]. Therefore, we incorporated MSC-Exos, successfully maintaining the transparency of the repaired cornea. Our results indicate that a combination of OGG/CMCS and MSC-Exos accelerates stromal healing and mitigates inflammation. Furthermore, this approach promotes collagen fiber regeneration and inhibits fibrosis.

While this study focused on corneal tissue, the versatility of the OGG/CMCS hydrogel combined with MSC-Exos suggests its potential for application in other tissues that require transparent scaffolding or surface integrity. Future studies could explore the use of this hydrogel system for treating other ocular surface injuries or extend its application to organs where transparent scaffolds and scarless healing are needed.

Conclusions

In conclusion, we developed an OGG/CMCS hydrogel from natural biopolymers featuring transparent, self-healing, injectable, and adhesive properties and it can promote corneal healing through MSC-Exos delivery. The hydrogel's formation through dynamic Schiff base interactions between OGG's aldehyde groups and CMCS's amino groups enabled tunable porosity, mechanical strength, and light transmittance by adjusting OGG concentrations. Notably, the hydrogel displayed remarkable self-healing and shear-thinning properties, facilitating smooth injection through a needle. Furthermore, it exhibited strong tissue adhesion at physiological

temperatures. Our experiments confirmed the MSC-Exos-loaded hydrogel can tightly adhere to the defected cornea, promote regeneration of corneal epithelium and stroma, inhibit corneal scarring, and mitigate inflammation. These findings underscore the hydrogel's scientific significance and clinical potential for corneal repair.

Supplementary Information

The online version contains supplementary material available at <https://doi.org/10.1186/s12951-025-03366-2>.

Supplementary Material 1

Author contributions

X.T.Z., M.Y.L., and B.K. conceived the idea and designed the experiment. All authors conducted experiments and data analysis; B.K. and R.Y.W. wrote the manuscript. R.L. contributed to the scientific discussion of the article. All authors reviewed the manuscript.

Funding

Shenzhen Medical Research Fund (B2401006 and A2303017), National Natural Science Foundation of China (82301251, 82371091, and 82201207), Guangdong Basic and Applied Basic Research Foundation (2024A1515010457), Shenzhen Science and Technology Program (JCYJ20240813175800001), Shanghai Yangfan Project (23YF1445300), Project of Shanghai Xuhui District Science and Technology (2020-015, XHLHGG202104), Shanghai Rising-Star Program (21QA1401500), Natural Science Foundation of Shanghai (23ZR1409200).

Data availability

The data that support the findings of this study are available from the corresponding author upon reasonable request.

Declarations

Competing interests

The authors declare no competing interests.

Received: 1 January 2025 / Accepted: 1 April 2025

Published online: 28 April 2025

References

- Mohan RR, Kempuraj D, D'Souza S, Ghosh A. Corneal stromal repair and regeneration. *Prog Retin Eye Res.* 2022;101090.
- Yao G, Mo X, Liu S, Wang Q, Xie M, Lou W, et al. Snowflake-inspired and blink-driven flexible piezoelectric contact lenses for effective corneal injury repair. *Nat Commun.* 2023;14:3604.
- Li Y, Wang Z. Biomaterials for corneal regeneration. *Adv Sci.* 2025;12:e2408021.
- Colby K. Update on corneal transplant in 2021. *JAMA.* 2021;325:1886–7.
- Jeng BH, Ahmad S. In Pursuit of the Elimination of Corneal Blindness: Is Establishing Eye Banks and Training Surgeons Enough? *Ophthalmology.* 2021;128:813–5.
- Alio JL, Montesal A, El Sayyad F, Barraquer RI, Arnalich-Montiel F, Alio Del Barrio JL. Corneal graft failure: an update. *Br J Ophthalmol.* 2021;105:1049–58.
- Li S, Ma X, Zhang Y, Qu Y, Wang L, Ye L. Applications of hydrogel materials in different types of corneal wounds. *Surv Ophthalmol.* 2023;68:746–58.
- Yan K, Zhang Q, Liu Q, Han Y, Liu Z. Advances in adhesive hydrogels applied for ophthalmology: an overview focused on the treatment. *Theranostics.* 2025;15:915–42.
- Zheng Y, Baidya A, Annabi N. Molecular design of an ultra-strong tissue adhesive hydrogel with tunable multifunctionality. *Bioact Mater.* 2023;29:214–29.
- Kang N-W, Jang K, Song E, Han U, Seo YA, Chen F, et al. In Situ-Forming, Bioorthogonally Cross-linked, Nanocluster-Reinforced hydrogel for the regeneration of corneal defects. *ACS Nano.* 2024;18:21925–38.
- Zhao L, Shi Z, Qi X, Wang J, Yu M, Dong M, et al. Corneal stromal structure replicating humanized hydrogel patch for sutureless repair of deep anterior-corneal defect. *Biomaterials.* 2025;313:122754.
- Kang N-W, Seo YA, Jackson KJ, Jang K, Song E, Han U, et al. Photoactivated growth factor release from bio-orthogonally crosslinked hydrogels for the regeneration of corneal defects. *Bioact Mater.* 2024;40:417–29.
- Sun X, Song W, Teng L, Huang Y, Liu J, Peng Y, et al. MiRNA 24-3p-rich exosomes functionalized DEGMA-modified hyaluronic acid hydrogels for corneal epithelial healing. *Bioact Mater.* 2023;25:640–56.
- Chang G, Dang Q, Liu C, Wang X, Song H, Gao H, et al. Carboxymethyl Chitosan and carboxymethyl cellulose based self-healing hydrogel for accelerating diabetic wound healing. *Carbohydr Polym.* 2022;292:119687.
- Zhang X, Liang Y, Huang S, Guo B. Chitosan-based self-healing hydrogel dressing for wound healing. *Adv Colloid Interface Sci.* 2024;332:103267.
- Bhujel B, Oh S-H, Kim C-M, Yoon Y-J, Kim Y-J, Chung H-S, et al. Mesenchymal stem cells and exosomes: A novel therapeutic approach for corneal diseases. *Int J Mol Sci.* 2023;24:10917.
- Li Y, Zhu Z, Li S, Xie X, Qin L, Zhang Q, et al. Exosomes: compositions, biogenesis, and mechanisms in diabetic wound healing. *J Nanobiotechnol.* 2024;22:398.
- Cao H, Duan L, Zhang Y, Cao J, Zhang K. Current hydrogel advances in physicochemical and biological response-driven biomedical application diversity. *Signal Transduct Target Ther.* 2021;6:426.
- Bertsch P, Diba M, Mooney DJ, Leeuwenburgh SCG. Self-Healing injectable hydrogels for tissue regeneration. *Chem Rev.* 2023;123:834–73.
- Fang W, Yang L, Chen Y, Hu Q. Bioinspired multifunctional injectable hydrogel for hemostasis and infected wound management. *Acta Biomater.* 2023;161:50–66.
- Zhu S, Dai Q, Yao L, Wang Z, He Z, Li M, et al. Engineered multifunctional nanocomposite hydrogel dressing to promote vascularization and anti-inflammation by sustained releasing of Mg²⁺ for diabetic wounds. *Compos Part B: Eng.* 2022;231:109569.
- Ren H, Zhang Z, Cheng X, Zou Z, Chen X, He C. Injectable, self-healing hydrogel adhesives with firm tissue adhesion and on-demand biodegradation for sutureless wound closure. *Sci Adv.* 2023;9:eadh4327.
- He L, Xing S, Zhang W, Wang Y, Li Y, Chen J, et al. Multifunctional dynamic chitosan-guar gum nanocomposite hydrogels in infection and diabetic wound healing. *Carbohydr Polym.* 2025;354:123316.
- Wang F, Zhang W, Qiao Y, Shi D, Hu L, Cheng J, et al. ECM-Like adhesive hydrogel for the regeneration of large corneal stromal defects. *Adv Healthc Mater.* 2023;12:e2300192.
- Wilson SE. Corneal myofibroblasts and fibrosis. *Exp Eye Res.* 2020;201:108272.
- Kumar A, Yun H, Funderburgh ML, Du Y. Regenerative therapy for the cornea. *Prog Retin Eye Res.* 2022;87:101011.
- Khosravimelal S, Mobaraki M, Eftekhari S, Ahearne M, Seifalian AM, Gholipour-malekabadi M. Hydrogels as emerging materials for cornea wound healing. *Small.* 2021;17:e2006335.
- Muir VG, Burdick JA. Chemically modified biopolymers for the formation of biomedical hydrogels. *Chem Rev.* 2021;121:10908–49.
- Kong B, Liu R, Cheng Y, Cai X, Liu J, Zhang D, et al. Natural biopolymers derived hydrogels with injectable, self-healing, and tissue adhesive abilities for wound healing. *Nano Res.* 2023;16:2798–807.
- Pandit AH, Nisar S, Imtiyaz K, Nadeem M, Mazumdar N, Rizvi MMA, et al. Injectable, Self-Healing, and biocompatible N,O-Carboxymethyl Chitosan/Multialdehyde Guar gum hydrogels for sustained anticancer drug delivery. *Biomacromolecules.* 2021;22:3731–45.
- Yin X, Hao Y, Lu Y, Zhang D, Zhao Y, Mei L, et al. Bio-Multifunctional hydrogel patches for repairing Full-Thickness abdominal wall defects. *Adv Funct Mater.* 2021;31:2105614.
- Du X, Wu L, Yan H, Jiang Z, Li S, Li W, et al. Microchannelled alkylated Chitosan sponge to treat noncompressible hemorrhages and facilitate wound healing. *Nat Commun.* 2021;12:4733.
- Lorenzo-Martín E, Gallego-Muñoz P, Mar S, Fernández I, Cidat P, Martínez-García MC. Dynamic changes of the extracellular matrix during corneal wound healing. *Exp Eye Res.* 2019;186:107704.
- Tan F, Li X, Wang Z, Li J, Shahzad K, Zheng J. Clinical applications of stem cell-derived exosomes. *Signal Transduct Target Therapy.* 2024;9:17.

Publisher's note

Springer Nature remains neutral with regard to jurisdictional claims in published maps and institutional affiliations.